INDENTATION SIZE EFFECT OF HEAT TREATED ALUMINUM ALLOY

Jozef Petrík[1)], Peter Blaško[1)], Andrea Vasilňaková[1)], Peter Demeter[1)], Peter Futaš[1)]*
[1)] *Technical University of Košice, Faculty of Materials, Metallurgy and Recycling, Košice, Slovakia*

Received: 09.07.2019
Accepted: 23.09.2019

**Corresponding author: e-mail:* jozef.petrik@tuke.sk, *Tel.: +421 55 602 2872, Institute of Materials and Quality Engineering, Faculty of Materials, Metallurgy and Recycling, Technical University of Košice, Letná 9, 042 00 Košice*.

Abstract
The aim of the submitted work is to study the influence of applied loads ranging from 0.09807 N to 0.9807 N on measured values of micro-hardness of heat treated aluminum alloy 6082. The influence of applied load on a measured value of micro-hardness was evaluated by Meyer's index n, PSR method and by Analysis of Variance (ANOVA). The influence of the load on the measured value of micro-hardness is statistically significant and the relationship between the applied load and micro-hardness manifests the moderate reverse ISE. As the temperature of the solution treatment rises, the YS/UTS ratio and also Meyer's index n, measured and "true hardness" increase. On the other hand, its effect on the plastic properties of the alloy is ambiguous.

Keywords: annealing, aluminium alloys, micro-hardness, ISE

1 Introduction

Aluminum alloys have been more and more extensively utilized in structural applications, aircraft, building and automotive industry due to their light weight and attractive mechanical properties achieved by heat treatment. In the Al-Mg-Si alloys the precipitation during aging after solution heat treatment and quenching significantly increase hardness and tensile strength.

Indentation hardness testing is a convenient means of investigating the mechanical properties of a small volume of materials. The principle of the Vickers micro-hardness method is identical to the macro-hardness test, except for considerably smaller test loads. It is frequently used for the determination of hardness of small items or thin layers [1].

In contrast to the (macro)hardness, it is well known that the apparent micro-hardness of solids depends on the load. This phenomenon, the indentation size effect (ISE), usually involves a modification in the apparent micro-hardness with a tenvariation of the load [2, 3].

If a very low load is used, the measured micro-hardness is usually high; with an increase in test load, the measured micro-hardness decreases. Such a phenomenon is sometimes referred to as "normal" ISE. Undoubtedly, the existence of the ISE may hamper or preclude plausible micro-hardness measurements [4]. The "normal" ISE may be caused by the testing equipment [1, 4, 5], the intrinsic structural factors of the material, load to initiate plastic deformation, indentation elastic recovery, elastic resistance of the materials, the effect of indenter/specimen friction resistance and the effect of the grinding and polishing of sample [1, 3-6].

In contrast to the above "normal" ISE, a reverse (inverse) type of ISE (RISE), where the apparent micro-hardness increases with increasing load, is also known. It essentially takes place in materials with predominant plastic deformation. It can be explained as an effect of vibration, indenter

DOI 10.12776/ams.v25i3.1310 p-ISSN 1335-1532
e-ISSN 1338-1156

bluntness at low loads, the energy loss as a result of sample chipping around the indentation or the generation of the cracks during the loading [3].
The purpose of this paper is to evaluate the influence of the load on micro-hardness of heat treated Al alloy 6082 by Meyer's, PSR and modified PSR methods. The scientific work devoted to the study of the influence of heat treatment on ISE is rare. This also applies to wrought aluminum alloys which, after forming, often follow heat treatment. The measurement of hardness and especially of micro-hardness is a suitable method of determining their mechanical properties, which has minimal material requirements and minimally damages the final product.

2 Experimental materials and methods

The investigation has been carried out on the aluminum Si – Mg – Mn alloy EN 6082 (STN 42 4400) which chemical composition (in wt.%) is in **Table 1.**

Table 1 The chemical composition of the alloy used for investigation.

Si	Mg	Mn	Fe	Cu	Ti	Cr
1.00	0.66	0.54	0.20	<0.03	<0.02	<0.02

The samples used for heat treatment had the shape of the cylinder with a length of 100 mm and a diameter of 16 mm. The samples were, after the solution treatment at temperatures listen in Table 2 with the holding time 3 hours quenched in the water. Then they were naturally aged for five days at 25°C. The sample No. 9 is the initial, hot extruded material used for heat treatment. One sample for the internaltensile test was turned for each temperature of the solution.
The temperature of heat treatment processes was measured by digital thermometer Testo 9010 with expanded uncertainty U = 2.3°C (k = 2) in calibration point 600°C.
The tensile test was carried out by the tester 200 kN Zwick-Extensometer according to standard ISO 6892-1:2016 [7]. The mean strain rate $\dot{e}_{Lc} = 0.024\ min^{-1}$. Results of the test are in **Table 2**. The experimental error expressed as relative expanded uncertainty U_{rel} (coverage factor k = 2) is 1.82 % for values UTS and YS and less than 1% for values TE and Z. The YS/UTS ratio, which controls the local loss of plastic stability due to the internal structure of material (non-homogeneity, defects, but also due to the processing technology) for example in the deep-drawing process. High value of the ratio results in restricted formability and resistance to fatigue fracture on the other hand [8, 9]. As the temperature of the solution treatment rises, the YS/UTS ratio and also Meyer's index n increase.

Table 2 The temperature of the solution treatment, results of tensile test, (marco)hardness (HV10), micro-hardness (HV 0.05) and the relative expanded uncertainty of the hardness (U_{rel})

sample	T (°C)	UTS [MPa]	YS [MPa]	TE [%]	Z [%]	YS/UTS	HV10	U_{rel} HV10 [%]	HV0.05	U_{rel} HV0.05 [%]
1	590	235	131	20.4	26.7	0.557	118	7.6	118	15.0
2	580	237	121	19.5	44.5	0.511	122	7.7	111	18.0
3	570	242	124	23.8	46.9	0.512	121	6.9	114	15.3
4	560	230	126	20.8	51.4	0.548	117	7.6	134	13.1
5	550	236	124	19.6	51.8	0.525	124	8.7	110	15.9
6	540	314	127	15.6	43.9	0.404	108	7.5	107	17.0
7	530	298	144	16.0	42.8	0.483	102	7.6	101	17.5
8	520	280	143	13.2	48.9	0.511	95	8.4	98	18.3
9	-	291	113	18.8	47.2	0.388	105	5.8	103	17.0

DOI 10.12776/ams.v25i3.1310 p-ISSN 1335-1532
e-ISSN 1338-1156

A head part of the longer fractured tensile piece was used as a sample for metallographic analysis and measurement of the macro- and micro-hardness. The diameter of the piece was measured at regular intervals from the neck to the head. Dimensions parallel to the axis of the sample are measured with an accuracy 0.01 mm and dimensions perpendicular to the axis with an accuracy 0.001 mm.

The surface was wet ground on silicon carbide papers (the sequence 80, 120, 220, … 2500 and 3000 ANSI/CAMI grit) and mechanically polished with a water suspension of Al_2O_3 and then with diamond paste (0.5 μm) to a mirror finish. Samples were finally etched with water solution 0.5 % HF. The etching visualized hard intermetallic phases, firstly Al-Fe. The areas with the occurrence of intermetallic phases were avoided at micro-hardness measurement.

The microstructure was analyzed by optic microscope Neophot 32 in magnifications 500 × and 1000×, using the software ImageJ. The aluminum matrix contains fine intermetallic particles which became visible after etching. The area of their proportion is 1.8 % in the initial material and it is between 0.8 % and 1.3 % in heat treated samples. The temperature of the solution treatment did not significantly affect this proportion.

The (macro)hardness tests were performed by the equipment HBO 250. The magnification of the measuring device is 70×. The certified reference material (CRM) in the form of hardness reference block with specified hardness H_c = 194 HV 10 and expanded uncertainty U_{CRM} = 3.3 HV 10 (k = 2) was used as a standard for the calibration of the tester; it met the requirements of the standard ISO 6507-2:2018 [10] (the repeatability r_{rel} = 1.94%, the error of tester E_{rel} = 0.20 % and the expanded uncertainty of the calibration (k = 2) U_{rel} = 1.07 %). Measured values of the (macro)hardness are in **Table 2**.

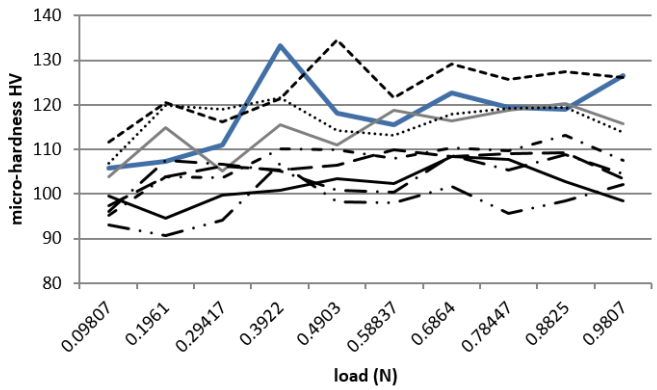

Fig. 1 The relationship between load and micro-hardness

Micro-hardness was measured by tester Hanemann, type Mod D32 fitted to microscope Neophot-32 with a magnification 480×. The discrimination - the value of the smallest division of the optical device, which measures the diagonals of the indentation, is 0.000313 mm.

A reference block – CRM (certified reference material) with specified hardness H_c = 195 HV0.05 and expanded uncertainty U_{CRM} = 8 HV 0.05 (k = 2) was used for the calibration of the micro-hardness tester; the tester meets the requirements of the standard ISO 6507-2:2018 [10] (r_{rel} = 4.39 %, E_{rel} = 3.81 % and U_{rel} = 9.01%).

Both macro- and micro-hardness were measured according to standard ISO 6507-1:2018 [11]. Applying load P for (macro)hardness was 98.07 N and loads for micro-hardness were between

DOI 10.12776/ams.v25i3.1310 p-ISSN 1335-1532
e-ISSN 1338-1156

0.09807 N and 0.9807 N by 0.09807 N step with application time 15 s. An operator performed five indentations at each load. For micro-hardness, the result was "the cluster" of 50 indentations, regularly distributed over the surface of the sample at one sample. If the measured micro-hardness was extremely high or the shape of the indentation was distorted, the indenter was likely contacted with the subsurface intermetallic phase. The measured value was not taken into account, and the measurement was repeated. The mean velocity of the micro-indenter in the sample, calculated by the method described in [12] was 1.0 μm s^{-1}. The values of micro-hardness, measured at particular loads are in **Fig. 1** and it at load 0.49 N (HV0.05) with its uncertainty are also in **Table 2**. As can be seen, the uncertainty of the micro-hardness is higher as it of (macro)hardness. It is the result of higher deviation of the diagonals of micro-indentations and at the same time higher uncertainty of used CRM (e. i. the ratio of CRM uncertainty and the hardness of tested aluminum alloy). The majority of samples manifest a moderate reverse indentation size effect (RISE). The ambient temperature in the laboratory ranged between 20.0 and 20.7 °C.

3 Results

According to two way analysis of variance (ANOVA, significance level $\alpha = 0.05$) without replication the load ($p = 3.52 \times 10^{-8}$) and the solution treatment temperature ($p = 6.32 \times 10^{-22}$) both have the statistically significant influence on the measured values of the micro-hardness.

Meyer's power law and proportional specimen resistance (PSR) are two principal approaches to describe ISE quantitatively [1].

The basic method to describe the ISE is Meyer's Law:

$$P = Ad^n \tag{1.}$$

Meyer's index n and the coefficient A (as A_{ln}) determined by the straight line graph of ln d (the mean diagonal of the indentation d in μm) versus ln P (the applied load P in g). Meyer's index n is the slope and coefficient A_{ln} is the y-intercept of the line.

Table 3 The ISE and PSR indices

method	Meyer's law		PSR		Modified PSR		
sample	n	A_{ln}	a_1 [N mm^{-1}]	a_2 [N mm^{-2}]	c_0 [N]	c_1[N mm^{-1}]	c_2 [N mm^{-2}]
1	2.1340	6.918	-1.686	690.08	0.0006	-1.677	689.06
2	2.1095	6.794	-1.559	662.82	0.0012	-1.722	666.68
3	2.0317	6.557	-0.100	621.03	-0.0421	3.635	548.08
4	2.1147	6.895	-1.458	711.51	-0.0326	1.455	653.41
5	2.1231	6.778	-1.355	618.36	-0.0543	3.157	534.63
6	2.0766	6.600	-0.676	586.11	-0.0787	5.824	466.64
7	2.0510	6.494	-0.541	572.17	0.0110	-1.412	587.68
8	2.0719	6.501	-0.787	546.11	-0.0183	0.708	519.19
9	2.0571	6.489	-0.615	560.98	-0.0903	6.650	430.71

However, as stated by a number of authors, for example, Sargent [13], presented the relationship between Meyer's index and work hardening coefficient was derived using the ball indenter. Unfortunately, it has become common practice to apply the strain-hardening Tabor interpretation to pyramidal indentation and to derive a "work-hardening index". The purpose of the contribution is not to give an opinion on whether the Meyer index is a measure of the work hardening coefficient or it is not. In this case, its task will only be to quantify the possible existence and magnitude of the relationship between load and microhardness, i.e. ISE.

DOI 10.12776/ams.v25i3.1310 p-ISSN 1335-1532
e-ISSN 1338-1156

The index n < 2 indicates "normal" and n > 2 indicates reverse ISE. If n = 2, the micro-hardness is independent of the load and is given by Kick's law.
The curves load/micro-hardness in **Fig. 1** show a non-linear increase of the micro-hardness with the applied load to 0.2942 – 0.4903N and then remain practically constant with further increasing of the load. This boundary of the stabilization as called as "ISE boundary". Calculated values of Meyer's index n and A_{ln} are in **Table 3**.
The proportional specimen resistance model of Li and Bradt (PSR) may be considered a modified form of the Hays/Kendall approach to the ISE [4]. Several authors [1, 4, 5, 14, 15] have proposed that the normal ISE may be described by the (2):

$$P = a_1 d + a_2 d^2 \tag{2.}$$

Li and Bradt pointed out that the parameters a_1 (N mm^{-1}) and a_2 (N mm^{-2}) of (2) are related to the elastic and plastic properties of the material, respectively [16].
The parameter a_1 characterizes the load dependence of micro-hardness and describes the ISE in the PSR model. It consists of two components: the elastic resistance of the test sample and the friction resistance developed at the indenter facet/sample interface [1, 5].
The parameter a_2 is directly related to the test sample's load-independent micro-hardness sometimes referred to as "true hardness" [4].
Equation (2) may be rearranged in the form:

$$\frac{P}{d} = a_1 + a_2 d \tag{3.}$$

The parameters a_1 and a_2 of (3) may be obtained from the plots of P/d (in N/mm) against d (in mm). Measured values of a_1 and a_2 are given in **Table 3**.
According to energy balance approach parameter c_0 is associated with residual surface stresses in the sample and parameters $c_1 \approx a_1$ and $c_2 \approx a_2$ are related, respectively with the elastic and plastic properties of the sample [1, 4].
Equation (4) can be regarded as a modified form of the PSR model.

$$P = c_0 + c_1 d + c_2 d^2 \tag{4.}$$

The parameters c_0 (N), c_1 (N mm^{-1}) and c_2 (N mm^{-2}) of (4) may be obtained from the quadratic regressions of P (in N) against d (in mm) and their measured values are given in **Table 3**.
The ratio c_1/c_2 (**Table 4**) is a measure of the residual stresses due to the machining and polishing of the sample while c_0 denotes the residual stresses in the sample. Therefore a relationship between c_0 and c_1/c_2 is expected [1], **Fig. 2**. With increasing macro and micro-hardness, the ratios a_1/a_2 and c_1/c_2 both decreases, c_0 and Meyer's index n increase.
Hays and Kendall proposed the existence of minimum test load W (N) necessary to initiate plastic deformation – the result is visible indentation. Only elastic deformation occurs below such load. In that event, the load dependence of hardness is expressed by equation (5):

$$P = W + A_1 d^2 \tag{5.}$$

Where A_1 (N mm^{-2}) is a constant independent of load. The values of W and A_1 may be obtained from the regressions of P (N) against d^2 (mm) [1]. The values of the indices obtained by modified PSR are given in **Table 4.** However, visible indentations (and so with plastic deformation) were created with the load 0.009807 N. This fact does not conform to the definition of parameter W.

DOI 10.12776/ams.v25i3.1310 p-ISSN 1335-1532
e-ISSN 1338-1156

Parameters a_2, c_2, and A_1 are directly related to load-independent micro-hardness sometimes referred to as "true hardness" H_{PSR} [1, 4, 5, 17].

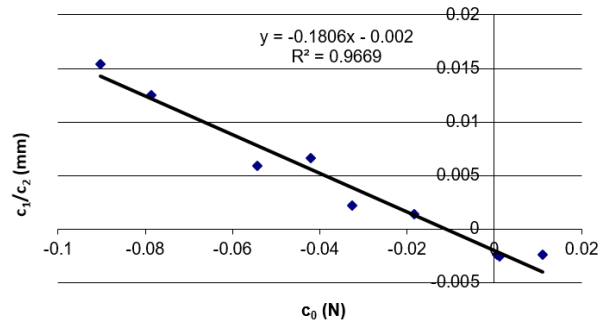

Fig. 2 The relationship between c_0 and c_1/c_2

$$H_{PSR}a_2 = 0.1891 \times a_2 \quad (6.)$$

The "true hardness" by analogy to a_2 can be calculated as H_{PSRA1} using A_1 and also $H_{PSR}c_2$ using c_2 in equation (6). The relationships between the ratio YS/UTS and "true hardness" calculated with the aid of the indices a_2, c_2 and A_1 and measured hardness HV0.05 and HV10 can be seen in **Fig. 3**. The coefficient of the determination R^2 ranged between 0.67 (for H_{PSRc2}) and 0.22 (for HV10).

Table 4 The ISE and PSR indices and "true hardness"

sample	W [N]	A1	c1/c2 [mm]	$\mathbf{H_{PSRa2}}$	$\mathbf{H_{PSRc2}}$	$\mathbf{H_{PSRA1}}$
1	-0.0200	658.01	-0.002430	130.4941	130.3012	124.4297
2	-0.0203	635.31	-0.002580	125.3393	126.0692	120.1371
3	0.0030	614.37	0.006633	117.4368	103.6419	116.1774
4	-0.0150	680.84	0.002226	134.5465	123.5598	128.7468
5	-0.0133	589.97	0.005904	116.9319	101.0985	111.5633
6	-0.0024	567.59	0.012481	110.8334	88.24162	107.3313
7	-0.0074	563.09	-0.002400	108.1973	111.1303	106.4803
8	-0.0088	531.09	0.001364	103.2694	98.17883	100.4291
9	-0.0012	543.48	0.015440	106.0813	81.44726	102.7721

4 Discussion

Parameter c_0 is associated with residual surface stress in the sample. It was assumed that the head part of the sample, used for ISE evaluation would not be significantly deformed. As can be seen in **Table 4** a certain difference in residual surface stress was observed. However, the mentioned differences were smaller than they obtained on a sample of the same material on the places with different local reduction of the area (contraction). Since the relationship between c_0 and the temperature of the solution treatment is negligible ($R^2 = 0.04$), the differences are likely the result of residual strain (for example, different deformations of heads when attached to the grips of the tensile machine). The ratio c_1/c_2 is the measure of the residual stress due to machining and polishing. Individual samples were sawn, ground and polished under approximately the same conditions. However, certain differences, which could cause differences in the values of c_1/c_2 ratio may have occurred (for example the polishing time or the contact force in the polishing or grinding). Hays and Kendall defined the parameter was a minimum load necessary to initiate

DOI 10.12776/ams.v25i3.1310 p-ISSN 1335-1532
e-ISSN 1338-1156

plastic deformation, therefore a creating a visible indentation. However, visible indentations (and so with plastic deformation) were created with the load 0.009807N, which is less than some calculated values of parameter W listed in **Table 4**. This fact does not conform to the definition of parameter W. It would be appropriate to focus the research on both of these problems in the future.

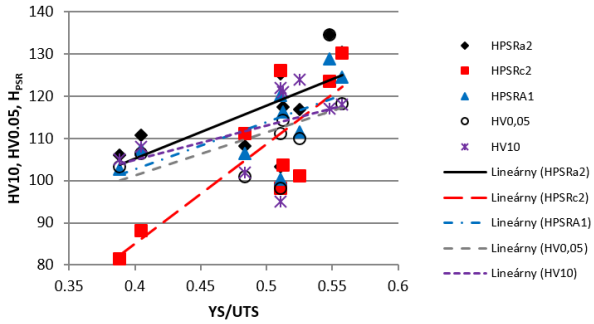

Fig. 3 The relationship between the YS/UTS ratio, "true hardness" HPSR and measured hardness HV0.05 and HV10

It is necessary to remember the fact that the indirect calibration of micro-hardness testers is not a routinely practiced process, unlike the (macro) hardness testers. We can determine the uncertainty of the measured micro-hardness only by the calibration. However, uncertainty can significantly affect the type and size of ISE. It is possible that "normal" and reverse ISE are simultaneously the result of the same input values if the uncertainty is taken into account (with a coverage factor k = 2) [18]. The ambiguity in the measurement of small indentations, particularly if pile-up or sink-in effects are present, can lead to over- or underestimation of diagonals [19, 20].

4 Conclusion

1. The influence of the load on the measured value of micro-hardness is statistically significant.
2. The relationship between the applied load and micro-hardness manifests moderate reverse ISE.
3. As the temperature of the solution treatment rises, the YS/UTS ratio and also Meyer's index n, measured and "true hardness" increase. On the other hand, its effect on the plastic properties of the alloy (reduction of the area Z and the elongation TS) is ambiguous.
4. The measured micro-hardness is effected by reverse ISE.

References

[1] K. Sangwal, B. Surowska, P. Błaziak: Materials Chemistry and Physics, Vol. 77, 2002, No. 2, p. 511-520, HTTPS://DOI.ORG/10.1016/S0254-0584(02)00086-X

[2] M. M. Yovanovich: *Micro and Macro Hardness Measurements, Correlations, and Contact Models*. In: 44th AIAA Aerospace Sciences Meeting and Exhibit, Reno, Nevada, 2006, http://www.mhtl.uwaterloo.ca/pdf_papers/mhtl06-2.pdf

[3] K. Sangwal: Materials Chemistry and Physics, Vol. 63, 2000, No. 2, p. 145-152, HTTPS://DOI.ORG/10.1016/S0254-0584(99)00216-3

[4] J. Gong, J. Wu, Zh. Guan: Journal of the European Ceramic Society, Vol. 19, 1999, No. 15, p. 2625-2631, https://doi.org/10.1016/S0955-2219(99)00043-6
[5] X. J. Ren, R. M. Hooper, C. Griffiths: Journal of Materials Science Letters, Vol. 22, 2003, No. 15, p. 1105-6, http://dx.doi.org/10.1023/A:1024947210604
[6] V. Navrátil, J. Novotná: Aplimat – Journal of Applied Mathematics. Vol. 2, 2009, No. 3, p. 241-244
[7] ISO 6892-1, Metallic materials - Tensile Testing. Part 1: Method of test at room temperature, ISO, Brussels, 2016
[8] A. Kováčová, T. Kvačkaj, R. Bidulský, J. Bidulská, R. Kočiško, J. Dutkiewicz, L. Lityńska-Dobrzyńska: Archives of Metallurgy and Materials, Vol. 62, 2017, Issue 2, p. 851-856, https://doi.org/10.1515/amm-2017-0125
[9] T. Kvačkaj, A. Kováčová, J. Bidulská, R. Bidulský, R. Kočiško: Archives of Metallurgy and Materials, Vol. 60, 2015, Issue 2A, p. 605-614, https://doi.org/10.1515/amm-2015-0180
[10] ISO 6507-2:2018 Metallic materials. Vickers hardness test. Part 2: Verification and calibration of testing, ISO, Brussels, 2018
[11] ISO 6507-1:20185 Metallic materials. Vickers hardness test. Part 1: Test method. ISO, Brussels, 2018
[12] J. Petrík, P. Palfy, P. Blaško, L. Girmanová, M. Havlík, Manufacturing technology. Journal for science, research and production Vol. 16, 2016, No. 4, p. 771-777, http://journal.strojirenskatechnologie.cz/templates/obalky_casopis/XVI_2016-4.pdf
[13] Ph. M. Sargent, Journal of materials science letters, Vol. 8, 1989, No. 10, p. 1139-1140, https://link.springer.com/article/10.1007/BF01730048
[14] H. Li, R. C. Bradt, Journal of Materials Science, Vol. 28, 1993, No. 4, p. 917-926, https://doi.org/10.1007/BF00400874
[15] B.D. Michels, G. H. Frischat, Journal of Materials Science, Vol. 17, 1982, No. 2, p. 329-334, https://doi.org/10.1007/BF00591466
[16] H. Kim, T. Kim, Journal of the European Ceramic Society, *Vol.* 22, 2002, No. 9-10, p**.** 1437-1445, https://doi.org/10.1016/s0955-2219(01)00457-5
[17] R. Machaka, T. E. Derry, I. Sigalas, M. Herrmann, Advances in Materials Science and Engineering, 2011, http://dx.doi.org/10.1155/2011/539252
[18] J. Petrik, P. Palfy: Metrology and measurement systems, Vol. 18, 2011, No. 2, p. 223-234, https://doi.org/10.2478/v10178-011-0005-5
[19] J. Petrík: Materials Science – Medžiagotyra, Vol. 20**,** 2014, No**.** 1, p. 21-24, http://dx.doi.org/10.5755/j01.ms.20.1.4017
[20] D. Tabor, Review of Physics in Technology, Vol. 1, 1970, No. 3, p. 145-179, https://doi.org/10.1088/0034-6683/1/3/I01

Acknowledgment
Authors are grateful for the support of experimental works by the project of the Slovak Grant Agency for Science VEGA 1/0073/17.